Implementation of an Entropy Closure Model for 2-D Hybrid Hall Thruster Simulations

Eunsun Cha, Mark A. Cappelli, and Eduardo Fernandez

***Abstract*— An entropy closure formulation for Hall thrusters was implemented in a radial–axial hybrid simulation. We modeled the entropy production and its scaling with effective collision frequency and magnetic field. This entropy source was used in an entropy transport equation resulting in a differential equation for the effective electron mobility. With this formulation, the effective electron mobility is a computed variable. This paper presents the results of 2-D hybrid simulations of a laboratory Hall thruster that incorporate this model and compares these results to simulations using both Bohm and experimental measurements for the mobility. Simulations were also performed using this model for varying discharge voltage and background gas density. The background gas density is found to have a significant effect on the computed discharge current. The entropy closure model is found to better capture the current–voltage characteristics that are measured experimentally than other models used for electron transport.**

***Index Terms*— Anomalous transport, entropy closure model, Hall-effect thrusters (HETs), propulsion, simulations.**

I. Introduction

THE Hall-effect thruster (HET) is a state-of-art technology for satellite station keeping, orbit maintenance, and orbit transfer. It has been widely studied by many researchers who have modified its traditional design for concepts that could make it suitable for various applications. Those applications include their use as high-power thrusters for a primary in-space propulsion system [1], air-breathing thrusters for low earth orbit missions, and hybrid engines that utilize the propellants that are shared with other on-board propulsion systems. The cost of xenon, which has increased significantly in recent years, has led to the development of HETs that operate on alternative propellants. Many researchers have expanded the propellant base to include iodine [2], [3], bismuth, krypton [4], nitrogen [5], and even air [6], [7].

Performance optimization of Hall thrusters and even design for alternative propellants will benefit from reliable computational tools because ground-based experiments and life testing are costly. In the Stanford Plasma Physics Laboratory (SPPL), we have been developing a 2-D hybrid particle-in-cell (PIC) simulation [8]. An important but poorly represented parameter in these simulations is the cross-field electron mobility, because establishing a reliable and stable model for the electron transport has been one of the greatest challenges in Hall thruster research. Measurements [9] of electron cross-field transport seem to imply that it is anomalously high—much higher than that described by classical collisions. Although models like those described by Bohm-type scaling with the magnetic field [10] are relatively straightforward to implement, they do not seem to capture the spatial variations in plasma properties throughout the Hall thruster channel. Early theories suggested the possible role played by electron–wall scattering in enhancing the so-called near-wall conductivity, although it appears that the loss of the high-energy electrons to the wall may not be replenished in the bulk plasma at a sufficient rate to account for the anomalous electron current. Researchers have used, with some success, *ad hoc* types of models with arbitrary coefficients or combinations of the early theories. However, the *ad hoc* models seem to be incapable of capturing plasma properties accurately, and often depend on some adjustable parameters derived from experiments. Thus, developing a suitable physical model for electron transport is one of the highest priorities for robust simulations of Hall thrusters because this would allow engineers to better explore their design space.

Recently, Knoll and Cappelli [11] developed a 1-D simulation that incorporated an isentropic description for the electron fluid. However, its implementation [12] into a 2-D simulation has been difficult for two reasons. First, the isentropic model has an inherently positive feedback characteristic, which hampers the convergence. Second, early results of simulations for a limited set of thruster conditions suggested the possible failure of the isentropic assumption in some regions of the thruster channel. In essence, the assumption of zero entropy production may not be valid in the regions where electron-scattering collisions are very frequent.

In this paper, we introduce a new method, which we refer to as an entropy closure model, to describe the electron transport in Hall thrusters. In this approach, we model the entropy production and its scaling with effective collision frequency, ν_{eff}, and magnetic field, B, and use a transport equation for electron entropy to close the set of equations for the electron fluid. The transport equation for electron entropy allows us to calculate the electron drift velocity, which defines the electron mobility in accordance with the electron momentum equation used in most of the Hall thruster simulations. Electron mobility, therefore, becomes a calculated parameter within the framework of a simulation.

Manuscript received December 1, 2013; accepted January 9, 2014. Date of publication February 4, 2014; date of current version January 6, 2015. This work was supported by the U.S. Air Force Office of Scientific Research.

E. Cha and M. A. Cappelli are with the Mechanical Engineering Department, Stanford University, Stanford, CA 94305 USA (e-mail: escha@stanford.edu; cap@stanford.edu).

E. Fernandez is with the Department of Mathematics and Physics, Eckerd College, St. Petersburg, FL 33711 USA (e-mail: fernane@eckerd.edu).

Color versions of one or more of the figures in this paper are available online at http://ieeexplore.ieee.org.

Digital Object Identifier 10.1109/TPS.2014.2304852

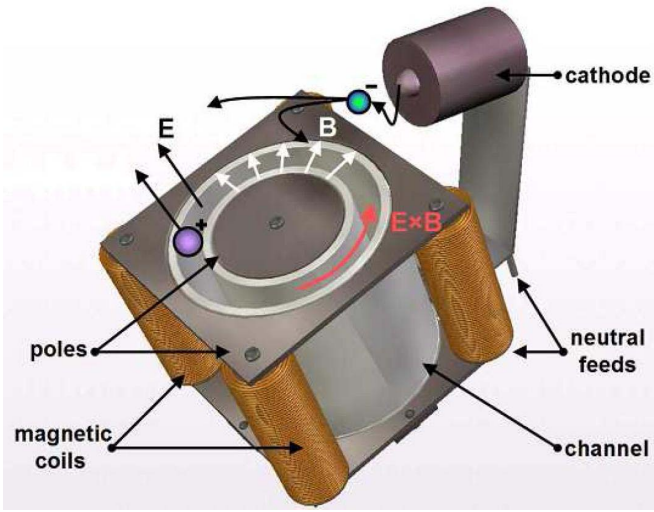

Fig. 1. Schematic view of the SHT [13].

In this paper, we implemented the entropy closure model in a laboratory Hall thruster [Stanford Hall thruster (SHT) schematically shown in Fig. 1] operating at 200 V. Section II provides the description of the numerical hybrid simulation and the entropy closure model, whereas Section III compares the results of the simulation to that using the experimental measurements as well as that using other transport models. To examine the transportability of the entropy closure model, simulations were carried out over a range of discharge voltages. In addition, the effects of background gas and the entropy loss due to heat transfer to the wall are discussed in Section III.

II. Numerical Model

A. Hall Thruster Simulation

The Hall thruster simulation used in this paper is built on the same simulation platform as that widely used by others in the SPPL. This initial simulation was developed in [8], and is similar to that of Fife at MIT [14]. The simulation uses the radial–axial plane of the Hall thruster as the computational domain. As shown in Fig. 2, the domain has an 8-cm-long channel that spans 1.2 cm in the radial direction. The imposed magnetic field, shown in Fig. 2, was based on the measurements made on the laboratory thruster.

The simulation is composed of a PIC component that pushes the heavy plasma constituents (ions and neutrals) and a fluid model for the lighter and magnetized electrons. These two components are coupled by quasi-neutrality ($n_e \approx n_i$). In the PIC component, each ion superparticle represents about 10^6–10^8 actual particles, while each neutral superparticle represents about 10^8–10^{10} actual particles. The computational domain is 2-D in the radial–axial plane, and we assume that the plasma properties are axisymmetric around the annulus of the Hall thruster. Despite this assumption of axisymmetry, the motion of the ions and neutrals is tracked in 3-D, whereas the electrons are treated as a quasi-1-D conducting fluid.

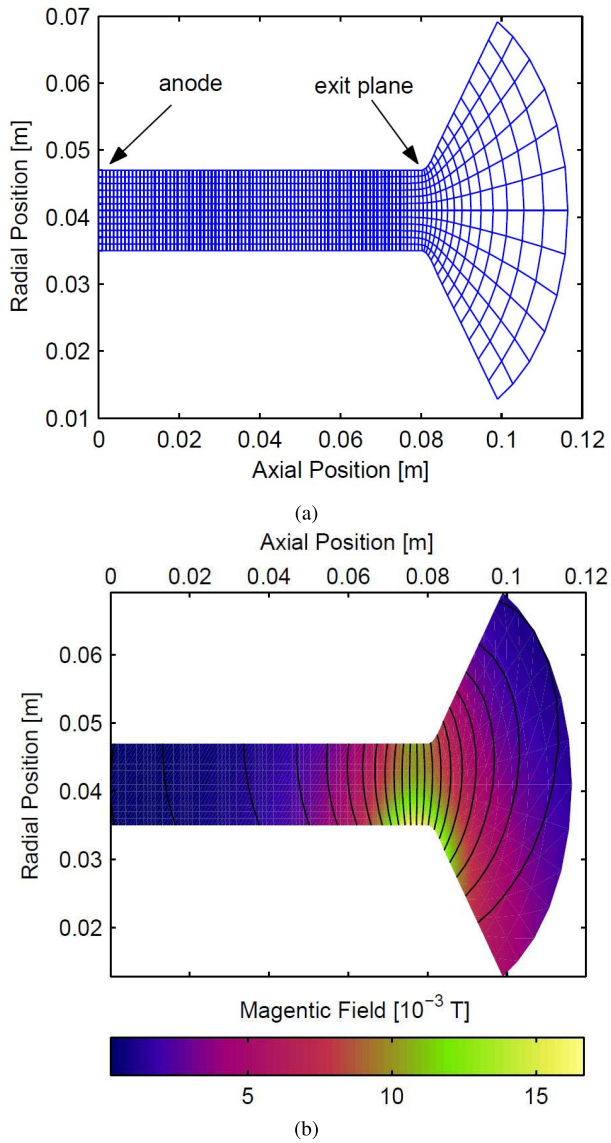

Fig. 2. (a) Radial–axial domain of the SHT depicting the grid used in these simulations. (b) Magnetic field.

Neutral superparticles are injected from the center of the anode based on the prescribed mass flow rate and are ionized by electron impact to produce singly ionized atoms/molecules. The ionization process is modeled as a function of electron temperature. This ion production serves as a source in the electron continuity equation as well as an energy drain in the electron energy equation. The energy lost through ionization includes cost factors to indirectly account for nonionizing collisions, which ultimately result in internal energy and radiation losses. The heavy particles are advanced in time through solution of their respective equations of motion in cylindrical coordinates. The background gas effect is also examined for the SHT simulation by applying a finite background gas pressure, 0.05 mTorr. Although previous research by our group examined the role played by charge exchange collisions [15], this effect is not included in the results presented in this paper. Further details about the simulation algorithm and the numerical scheme can be found in [16].

B. Entropy Closure Model

The entropy closure model is based on the assumption that in the regions of strong magnetic field, effective electron scattering collisions are less frequent, thus the rate of entropy production is expected to be small [17]. Using dimensional reasoning, this assumption guides the selection of a maximal set of parameters to determine the dimensionless relation that governs the local-scaled entropy production, $\dot{s}_e/k_B$. The set includes the plasma density, n_e, the effective collision frequency, ν_{eff}, the applied magnetic field, and B (through $\omega_{\text{ce}} = eB/m$). The scaling analysis leads us to the following relation:

$$\dot{s}_e = n_e k_B \nu_{\text{eff}} \cdot f\left(\frac{\omega_{\text{ce}}}{\nu_{\text{eff}}}\right). \tag{1}$$

The functional dependence of f must be determined by empirical means or theory, but we will test the simplest of unctions in this paper—one that is linear in the inverse Hall parameter

$$f\left(\frac{\omega_{\text{ce}}}{\nu_{\text{eff}}}\right) \approx \alpha \frac{\nu_{\text{eff}}}{\omega_{\text{ce}}} \tag{2}$$

where α is a constant. Equation (2) suggests a dependence of the entropy production rate on the square of the electron scattering frequency. Such a dependence is consistent with turbulence modeling, which leads to a dependence of the energy cascade rate from large to small structures on the square of the turbulence strain rate. In this reasoning, we postulate that the effective electron scattering is a result of scattering off of large-scale turbulent structures, which have characteristic fluctuation frequencies that scale inversely with the large eddy turnover times. In this paper, we take α to be of order of unity. α can be adjusted, if necessary, to best agree with the measured transport upstream of the peak magnetic field region.

A transport equation (3) for entropy, s_e, is used to close the set of equations for the electron fluid, where the existing set of equations are the first three moments of the Boltzmann equation

$$\frac{\partial(n_e s_e)}{\partial t} + \nabla \cdot n_e s_e \vec{u}_e = -\nabla \cdot \frac{\vec{q}_e}{T_e} + \dot{s}_e. \tag{3}$$

Here, T_e is electron temperature and $\vec{q}_e$ is the heat flux term

$$\vec{q}_e = -K_{\text{eff}} \nabla T_e \tag{4}$$

where it is expressed in terms of the effective thermal conductivity

$$K_{\text{eff}} = \frac{8 n_e k_B^2 T_e \mu_{\text{eff}}}{\pi e}. \tag{5}$$

Here, we examine two different approaches to the heat flux term in (3). In the initial implementation of the entropy closure model, we assume that the heat flux term is primarily axial (along a direction normal to the magnetic field contours). We compare this with the case where we include the entropy transfer to the walls by modeling the heat flux to the wall along the magnetic field contours.

Together with (1) and (2), the entropy transport (3) can be shown [17] to reduce to the following first-order ordinary differential equation for μ_{eff} for a 1-D simulation in which properties are assumed to vary mainly along the direction normal to the magnetic contour, i.e., along the $\hat{n}$ direction

$$\frac{8}{\pi}\frac{k_B T_e}{e}\frac{\partial \ln T_e}{\partial \hat{n}}\frac{d\mu_{e\text{eff}}}{d\hat{n}} + \frac{eB^3}{m_e}\mu_{e\text{eff}}^2 + \beta\,\mu_{e\text{eff}} - \frac{\dot{n}_e s_e}{k_B n_e} - \frac{q_{ew}}{L k_B T_e n_e} = 0. \tag{6}$$

Here, $\dot{n}_e$ is the ionization rate, q_{ew} is heat flux to the wall, and L is the contour length. The variable β in (6) is

$$\beta = \frac{k_B T_e}{e}\left[\frac{eE}{k_B T_e} + \frac{d\ln n_e}{d\hat{n}} + \frac{d\ln T_e}{d\hat{n}}\right]\left[\frac{3}{2}\frac{d\ln T_e}{d\hat{n}} - \frac{d\ln n_e}{d\hat{n}}\right] + \frac{8}{\pi}\frac{k_B T_e}{e}\left[\frac{d\ln T_e}{d\hat{n}}\frac{d\ln n_e}{d\hat{n}} + \left(\left(\frac{d\ln T_e}{d\hat{n}}\right)^2 + \frac{d^2\ln T_e}{d\hat{n}^2}\right)\right]. \tag{7}$$

Further details about the theoretical background and the derivation of the entropy model can be found in [17].

C. Implementation

There are several possible approaches to the numerical application of (6) to the hybrid simulation. In this paper, we chose to solve a quadratic equation for $\mu_{e\text{eff}}$ by setting the first order derivative, $d\mu_{e\text{eff}}/d\hat{n}$, to a constant at the given timestep and equal to that determined by the previous timestep. With this numerical strategy, we benefit in two ways. First, the computation cost is significantly reduced, because no iteration is necessary for each node at each timestep. Second, and more importantly, we avoid the challenging singularity problem that is caused by the structure of the coefficient to the first-order derivative of $\mu_{e\text{eff}}$. The analysis of [17] shows that the contribution to the resulting mobility from the first-order derivative term is small, justifying this approach.

Equation (6) is solved along the centerline of the radial dimension and use it as a representative value for each axial position for the purposes of both numerical stability and cost efficiency. The derivatives of the logarithms of electron temperature and density ($d\ln T_e/d\hat{n}$, $d\ln n_e/d\hat{n}$) are calculated using a second-order Newton's method at each timestep, with the computed data from the previous timestep.

Numerical adjustments were adopted after a series of preliminary studies with the entropy closure model to enhance the stability. These include attention to the region close to the anode when using the effective mobility as calculated by (6). In our current version of this hybrid simulation, the computational grid near the anode is not well resolved due to the small variations in the magnetic field in this region. This led to some numerical instability, which was avoided by enforcing the classical mobility in that region. In the rest of the domain, the computed mobility is introduced gradually at each time step, with 10% of the instantaneously computed mobility at each timestep added to 90% of the mobility used in the previous timestep. The instantaneously computed mobility is also filtered by local averaging to reduce high-frequency spatial noise.

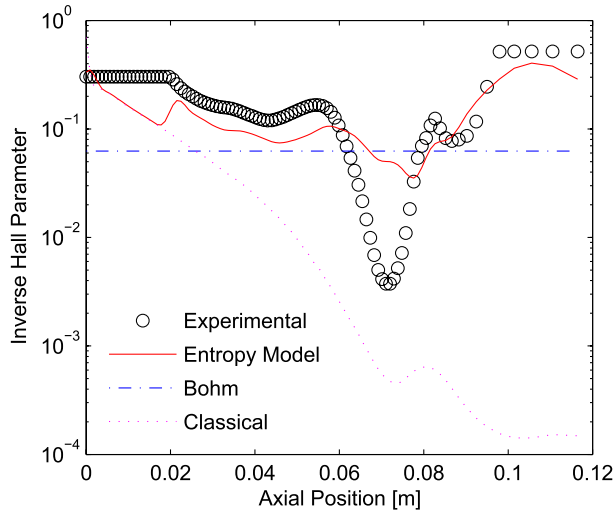

Fig. 3. Simulated inverse Hall parameter computed using the entropy closure model (red solid line) and compared with (a) experimentally measured values (open circles), (b) values based on a Bohm model (blue dashed line), and (c) computed value using classical theory (red dotted line). The discharge voltage is 200 V. Background gas and entropy wall loss are not accounted for in these simulations. Xenon mass flow of 2 mg/s is used for all cases.

III. Results and Discussion

A. Comparison of Transport Models

A representative example of the entropy closure model performance in the hybrid simulation for the SHT is shown in Fig. 3. The time-averaged profiles of the computed inverse Hall parameter and the effective mobility are compared to the experimentally measured data, a Bohm model, and the transport computed based on classical scattering. The nominal operating condition for the SHT is used (discharge voltage of 200 V and the xenon mass flow rate of 2 mg/s). The calculated electron transport using the entropy closure model captures the transport barrier, although weak, near the exit plane (where the axial position is 0.08 m) and agrees reasonably well with that measured at the axial positions between 0.02 and 0.04 m and outside the channel where the axial position is greater than 0.08 m.

Fig. 4 shows a comparison of the axial profiles of the simulated potential, electron temperature, and plasma density to those measured experimentally. The entropy closure model predicts the potential drop in the acceleration region to be more gradual than that observed in the experimental measurements. This is consistent with the weaker transport barrier generated using the entropy closure model. The model-simulated electron temperature is observed to be approximately 50% higher at the peak than those measured experimentally. However, the location of this computed peak is closer to the peak location measured experimentally than is the peak location computed using the Bohm model.

B. Background Gas Effect

Table I compares the simulated discharge currents to the experimental measurement at 200 V. The discharge current computed using the entropy closure model is 1.84 A.

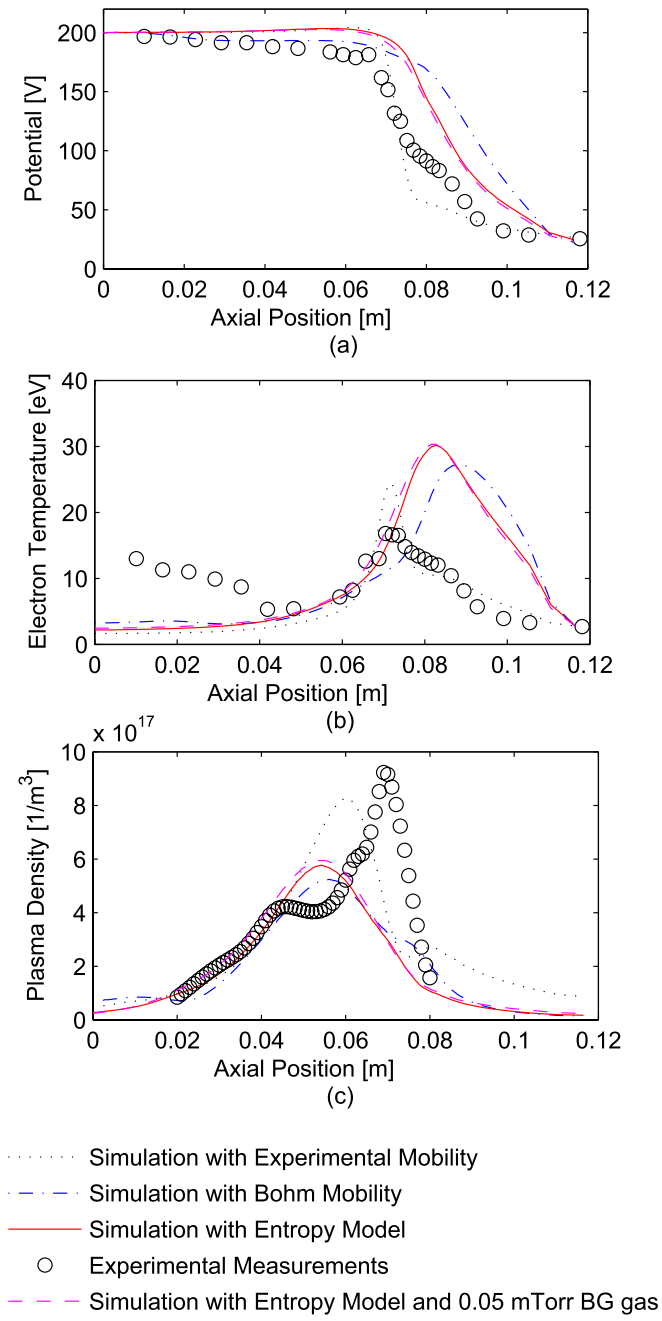

Fig. 4. Comparison of the experimental measurements of plasma properties with results of simulations using Bohm, experimental, and entropy models for the mobility. The discharge voltage is 200 V. (a) Plasma potential. (b) Electron temperature. (c) Plasma density.

This value is close to that computed using the Bohm and classical models. However, when the effect of background gas is included (0.05 mTorr), the computed discharge current increases slightly to 2.21 A, and when the entropy wall loss term is included, the current increases up to 2.34 A. This background effect is clearly observed from the current–voltage (I–V) characteristics over the discharge voltage range from 100 to 200 V in Fig. 5. Fig. 5 compares the I–V characteristics computed by the entropy closure model to that measured experimentally, as well as that computed using the experimentally measured mobility. It is noteworthy that the

TABLE I
COMPARISON OF SIMULATED AND EXPERIMENTALLY MEASURED DISCHARGE CURRENT. DISCHARGE VOLTAGE IS 200 V. BACKGROUND GAS PRESSURE IS 0.05 mTorr IF APPLICABLE

	Discharge Current [A]
Experimental Measurement	2.7
Simulation with Entropy Model (no wall loss)	1.84
Simulation with Entropy Model (no wall loss) and Background Gas	2.21
Simulation with Entropy Model (wall loss included) and Background Gas	2.34
Simulation with Experimental Mobility	1.88
Simulation with Bohm Mobility	1.75

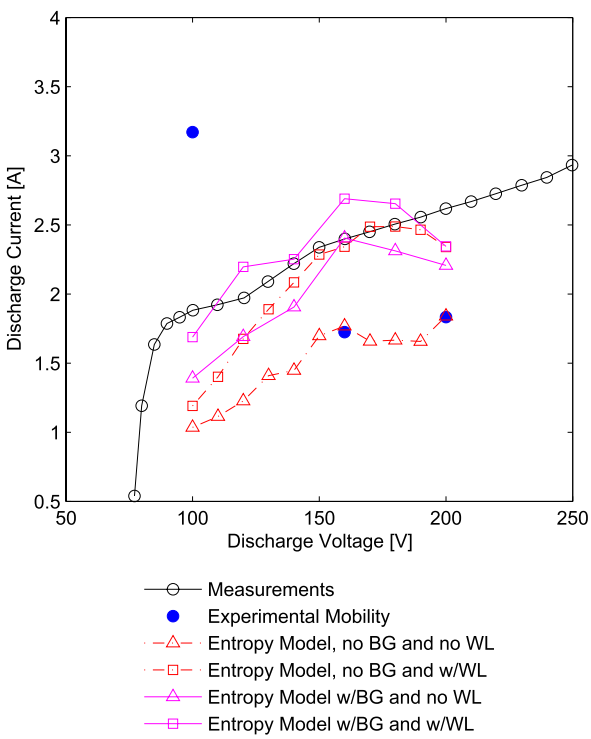

Fig. 5. Comparison of discharge voltage and current characteristics. The xenon mass flow is 2 mg/s and the background gas pressure is 0.05 mTorr if applicable.

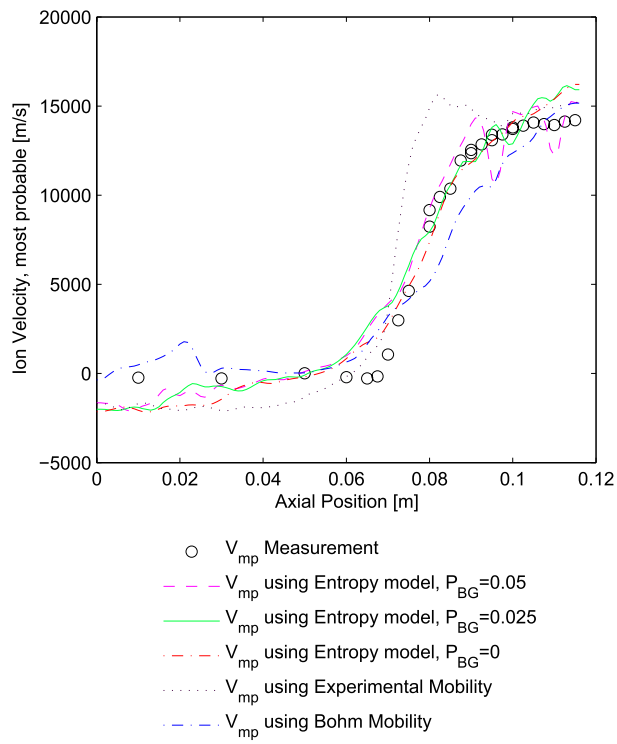

Fig. 6. Comparison of the measured most probable ion velocity most probable ion velocities simulated using the various models for experimental mobility. Various background pressures and the entropy wall loss were included in cases computed using the entropy closure model. The discharge voltage is 200 V and a xenon mass flow of 2 mg/s are used for all cases.

I–V characteristics predicted by the entropy closure model show a trend similar to that obtained in the experiments. This trend is not observed when the measured mobility is used in the simulations, particularly for the low discharge voltage cases.

While background gas does not significantly affect the simulated plasma properties, such as electron temperature and plasma density (Fig. 4), it influences the axial ion velocity, as shown in Fig. 6.

Fig. 6 compares the simulated ion velocities using the entropy closure model to the ion velocities simulated using various transport models and the experimental measurements. Note that because the experimental ion velocity data (○) are the most probable values from laser-induced fluorescent velocimetry [18], we used the ion data from simulations to sample the most probable ion velocities at each axial position. The entropy model prediction for the axial ion velocity is in remarkably good agreement with the measurements, especially at the axial location between 0.03 and 0.1 m, when compared with the simulated results using other transport models, such as the experimental mobility and Bohm mobility. This is encouraging, considering that the ion velocity measurements carry some of the smallest experimental uncertainty. With zero or lower background pressure of 0.025 mTorr, the entropy model predicted the ion velocity to be slightly higher than the measurements at the plume region (outside the channel). When the background pressure is increased up to 0.05 mTorr, the number of ions with lower speeds increases.

C. Entropy Wall Loss

Inclusion of the heat conduction wall loss in the entropy model seems to increase the resulting entropy production and

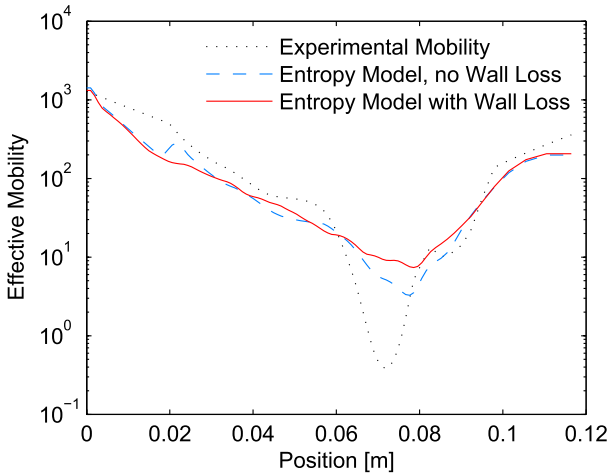

Fig. 7. Effective electron mobility simulated using the entropy model (with and without the wall loss contribution) are compared with the experimentally measured mobility. Background gas is not included. A discharge voltage of 200 V and xenon mass flow of 2 mg/s are used for all cases.

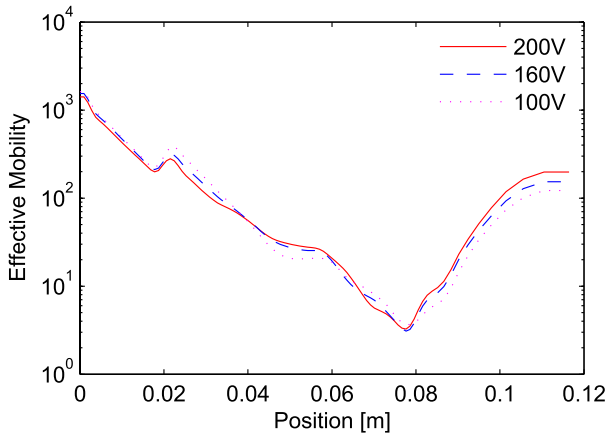

Fig. 8. Comparison of the simulated mobility using the entropy model at various discharge voltages. The background gas effect and entropy wall loss are not included in this comparison. A xenon mass flow of 2 mg/s is used for all cases.

enhance the computed electron transport in regions of the plasma near the ionization zone (Fig. 7). Increased entropy production is expected since it must compensate for the entropy lost to the wall. As a consequence of this increased entropy source rate, the discharge current increases substantially over the entire operating voltage range considered, as shown in Fig. 5. This finding substantiates the importance placed on radial conduction losses (not only for energy, but also for entropy), requiring that 1-D modeling of Hall thrusters should also include these important losses, at the very least, in *ad hoc* ways.

D. Discharge Voltage Variation

Discharge voltages other than the nominal 200 V were tested to study the portability of the closure model. The computed mobility for 100, 160, and 200 V are compared in Fig. 8, which shows that the mobility calculated with the entropy closure model is not very sensitive to the discharge voltage. This is despite the fact that the calculated plasma properties (and their spatial variation) do seem to vary, albeit weakly, with the change in discharge voltage. This is expected from the nature of the derived mobility equation because the effective mobility depends on the logarithms of plasma density and electron temperature. This result suggests that for any given thruster, it may be possible to find a universal curve (for a given magnetic field configuration) that captures the general transport behavior. Such a universality is embedded in the Bohm model description, where the mobility is inversely proportional to the magnetic field through a constant of O (0.05).

IV. Conclusion

This paper describes the introduction of an entropy closure model into hybrid simulations of Hall thrusters. The model uses dimensional scaling guided by the experiments to prescribe the rate of entropy produced due to effective electron scattering and uses this rate in an entropy transport equation to close the set of equations for the electron fluid. The entropy transport equation removes the need to provide an independent specification of the electron mobility because it falls out of the simulations as a computed property. We compared the performance of this model to the experimental measurements conducted on the SHT and also to the simulated results using the experimental mobility and a commonly used Bohm mobility. This entropy closure model is found to perform as well as simulations carried out using the experimentally measured mobility, and in some operating regions (e.g., low voltage), better captures the trends in discharge current observed experimentally. The wall loss effect as well as the background gas increased the simulated discharge current. However, the simulated mobility using the entropy model was not very sensitive to the operating conditions, such as background pressure, and discharge voltages. Future work will include studies of how well this model predicts the performance of other xenon-fueled Hall thrusters, such as the SPT-100, as well as thrusters operating on alternative propellants.

References

[1] C. R. Koppel and D. Estublier, "The SMART-1 Hall effect thruster around the moon: In flight experience," in *Proc. 29th Int. Electr. Propuls. Conf.*, 2005, pp. 1–9.

[2] A. C. Hillier, *Revolutionizing Space Propulsion Through the Characterization of Iodine as Fuel for Hall-Effect Thrusters*. Patterson, OH, USA: Air Force Inst. Technol., 2011.

[3] (2013, Sep.). *Hall Effect Thrusters* [Online]. Available: http://www.busek.com/technologies__hall.htm

[4] D. B. Scharfe, "Alternative hall thruster propellants krypton and bismuth: Simulated performance and characterization," Ph.D. dissertation, Dept. Mech. Eng., Stanford Univ., Stanford, CA, USA, 2009.

[5] E. Cha, M. A. Cappelli, and E. Fernandez, "Hybrid simulations of Hall thruster operating on various propellants," in *Proc. 31st Int. Electr. Propuls. Conf.*, 2009, pp. 2009–075.

[6] G. Cifali, P. Rossetti, M. Andrenucci, M. Valentine, D. Feili, and B. Lotz, "Experimental characterization of HET and RIT with atmospheric propellants," in *Proc. 32nd Int. Electr. Propuls. Conf.*, 2011, pp. 2011–224.

[7] L. Garrigues, "Study of a hall effect thruster working with ambient atmospheric gas as propellant for low earth orbit missions," in *Proc. 32nd Int. Electr. Propuls. Conf.*, 2011, pp. 1–12.

[8] E. Fernandez, M. A. Cappelli, and K. Mahesh, "2D simulations of hall thrusters," in *Proc. Center Turbulance Res. Annu. Res. Briefs*, 1998, pp. 81–90.

[9] N. B. Meezan, W. A. Hargus, and M. A. Cappelli, "Anomalous electron mobility in a coaxial Hall discharge plasma," *Phys. Rev. E*, vol. 63, p. 026410, Feb. 2001.

[10] D. Bohm, E. Burhop, and H. Massey, *The Characteristics of Electrical Discharges in Magnetic Fields*. New York, NY, USA: McGraw-Hill, 1949.

[11] A. K. Knoll and M. A. Cappelli, "A simple isentropic model of electron transport in Hall thrusters," *J. Phys. D. Appl. Phys.*, vol. 41, no. 16, pp. 162003-1–162003-6, Aug. 2008.

[12] E. Cha, M. A. Cappelli, and E. Fernandez, "Implementation of a polytropic model for two-dimensional hybrid Hall thruster simulations," in *Proc. 65th Annu. Gaseous Electron. Conf. Bull. Amer. Phys. Soc.*, vol. 57. 2012, p. 51.

[13] C. A. Thomas, "Anomalous electron transport in the Hall-effect thruster," Ph.D. dissertation, Dept. Mech. Eng., Stanford Univ., Stanford, CA, USA, 2006.

[14] J. M. Fife, "Nonlinear hybrid-PIC modeling and electrostatic probe survey of Hall thrusters," Ph.D. dissertation, Dept. Aeronautics Astronautics, Massachusetts Inst. Technol., Cambridge, MA, USA, 1998.

[15] M. K. Allis, N. Gascon, M. A. Cappelli, and E. Fernandez, "Effect of charge exchange on 2D Hall thruster simulation," in *Proc. 29th Int. Electr. Propuls. Conf.*, 2005, 1–12.

[16] M. K. Scharfe, "Electron cross field transport modeling in radial-axial hybrid Hall thruster simulations," Ph.D. dissertation, Dept. Mech. Eng., Stanford Univ., Stanford, CA, USA, 2009.

[17] M. A. Cappelli, E. Cha, and E. Fernandez, "Entropy closure model for transport in Hall thruster simulations," in *Proc. 33rd Int. Electr. Propuls. Conf.*, 2013, pp. 2013–088.

[18] W. A. Hargus, "Investigation of the plasma acceleration mechanism within a coaxial Hall thruster," Ph.D. dissertation, Dept. Mech. Eng., Stanford Univ., Stanford, CA, USA, 2001.

Eunsun Cha received the B.S. and M.S. degrees in mechanical and aerospace engineering from Seoul National University, Seoul, Korea, in 2003 and 2005, respectively. She is currently pursuing the Ph.D. degree in mechanical engineering with Stanford University, Stanford, CA, USA.

Her current research interests include improving Hall thruster simulations, in particular, the areas of electron transport, as well as running and modeling Hall thrusters with molecular propellants like nitrogen.

Mark A. Cappelli received the B.A.Sc. degree in physics from McGill University, Montreal, QC, Canada, and the M.A.Sc. and Ph.D. degrees in aerospace science and engineering from the University of Toronto, Toronto, ON, Canada, in 1980, 1983, and 1987, respectively.

He is currently a Professor with the Department of Mechanical Engineering, Stanford University, Stanford, CA, USA. His current research interests include the broad aspects of plasmas and gas discharges as they apply to aerodynamic and space propulsion, combustion, electromagnetics, and material processing.

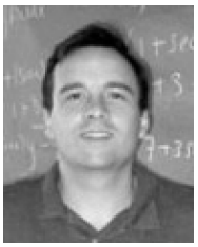

Eduardo Fernandez received the B.S. degree in physics and mathematics, and the Ph.D. degree in physics from the University of Wisconsin-Eau Claire, Eau Claire, WI, USA.

He is currently a Professor of Physics and Mathematics with Eckerd College, St. Petersburg, FL, USA. His current research interests include in the area of plasma physics, in particular, the simulation of magnetized, low-temperature plasmas used in electric propulsion applications, and turbulence in fusion plasmas.